

# SYNTHESIS OF Fe-BTC/GO NANO COMPOSITE BY HYDROTHERMAL METHOD WITHOUT USING ORGANIC SOLVENT

TỔNG HỢP NANO COMPOZIT Fe-BTC/GO BẰNG PHƯƠNG PHÁP THỦY NHIỆT KHÔNG DÙNG DUNG MÔI

Vũ Thị Hòa<sup>1\*</sup>, Lê Hà Giang<sup>2</sup>,  
Vũ Minh Tân<sup>1</sup>, Vũ Anh Tuấn<sup>2</sup>

## ABSTRACT

An Fe-BTC/graphene oxide (GO) composite was successfully synthesized by hydrothermal method. The samples were characterized by X-ray diffraction (XRD), energy-dispersive X-ray spectroscopy (EDX), N<sub>2</sub> adsorption-desorption (BET), transmission electron microscopy (TEM), fourier transform infrared spectroscopy (FTIR). The as-prepared Fe-BTC/GO nanocomposite was tested the photocatalytic degradation of reactive dye (reactive red-RR195) in aqueous solution. The Fe-BTC/GO composite exhibited excellent photocatalytic activity. The research suggested a potential application of Fe-BTC/GO composite as a highly efficient photocatalytic degradation of reactive dye in aqueous solution.

**Keywords:** Fe-BTC/GO composite, hydrothermal method, photocatalytic degradation, simulated sunlight irradiation.

## TÓM TẮT

Vật liệu composit kết hợp giữa Fe-BTC và graphen oxit được tổng hợp bằng phương pháp thủy nhiệt. Các mẫu vật liệu được đặc trưng bởi phương pháp nhiễu xạ tia X (XRD), phương pháp phổ tán xạ năng lượng tia X (EDX), phương pháp hấp phụ và khử hấp phụ N<sub>2</sub> (BET), phương pháp kính hiển vi điện tử truyền qua (TEM), phương pháp phổ hồng ngoại (FTIR). Vật liệu nano composit Fe-BTC/GO được thử nghiệm khả năng phân hủy quang xúc tác thuốc nhuộm (RR195) trong dung dịch nước. Vật liệu này thể hiện tốt khả năng làm xúc tác quang hóa. Điều này mở ra một tiềm năng ứng dụng của vật liệu Fe-BTC/GO trong phân hủy quang xúc tác thuốc nhuộm hoạt tính trong dung dịch nước.

**Từ khóa:** Vật liệu composit Fe-BTC/GO, phương pháp thủy nhiệt, phân hủy quang xúc tác, chiếu xạ ánh sáng mô phỏng.

<sup>1</sup>Trường Đại học Công nghiệp Hà Nội

<sup>2</sup>Viện Hóa học, Viện Hàn lâm Khoa học và Công nghệ Việt Nam

\*Email: vuthihoa76@hau.edu.vn; vuthihoa100276@gmail.com

Ngày nhận bài: 25/8/2018

Ngày nhận bài sửa sau phản biện: 22/10/2018

Ngày chấp nhận đăng: 25/10/2018

## 1. INTRODUCTION

Metal-organic frameworks (MOFs) are a new class of hybrid materials assembled with a metal cation and

organic linker, and have received great attention in recent years due to their unique properties of high surface area, crystalline open structures, functionality, and use in separation, gas storage, adsorption, and catalysis[1-5]. Several MOFs consisting of an Fe(III) oxo cluster, linked together by organic ligands, are highly photocatalytic due to their small Fe(III) oxo cluster size limiting the electron hole recombination, and their sensitive optical response in visible light [6,7]. Graphene oxide (GO) is a functionalized graphene with varying oxygen-containing groups such as hydroxyl, carboxylic, carbonyl, and epoxide groups. Several research groups have reported the formation of composite materials in which chemical bonds between the MOF and other substrates are involved [8-10]. Petit et al [11, 12] reported the formation of MOF/GO composites via interactions between the oxygen groups of GO and the metal centers of the MOF. This is responsible for enhancing the adsorption capacity of toxic gases like NH<sub>3</sub>, H<sub>2</sub>S, and NO<sub>2</sub>. However, composites of MOFs with graphene-based materials (GO and graphene) as highly efficient photocatalysts have rarely been explored until now. In the present work, we report the synthesis, characterization and application of this novel Fe-BTC/GO composite as a highly efficient photocatalyst in the degradation of reactive dye (reactive red-RR195).

MOF materials was synthesized by many method such as: solvothermal method, electricization, micro ware, ultrasling. However, these methods have some disadvantages, such as high energy cost, multiple minor products, low of the synthesized materials. In this paper, we report herein the synthesis of composite materials (Fe-BTC/GO) by hydrothermal method which is considered to be environmentally friendly and energy saving.

## 2. EXPERIMENTAL

### 2.1. Synthesis of GO

GO was prepared by chemical oxidation of natural graphite to form graphite oxide using a modified Hummers

method [13]. Graphite oxide powders were exfoliated by treatment in a microwave oven (Model MWO-G20SA, power 700W) for 1 min[14]. Upon microwave irradiation, we observed much larger volume expansion of the GO powders compared to that of GO obtained by exfoliation using ultrasonic treatment.

## 2.2. Synthesis of Fe-BTC/GO composite by hydrothermal method

At the first stage, 2.26 g of iron(II) chloroatetrahydrate ( $\text{FeCl}_2 \cdot 4\text{H}_2\text{O}$ ) was put into 97.2 ml  $\text{H}_2\text{O}$  and stirred to form solution (1). After that, 1.68 g of  $\text{H}_3\text{BTC}$  was added into 23.72 g of a 1M NaOH solution using magnetic stirrer to form solution (2). At the second stage, the solution (2) was transferred gradually to solution (1) and the mixture was stirred until the color of the liquid turns from green to brown (about 1 hour). At the third stage, 0.8 g GO was put into the stirring mixture and stirred for about 30 minutes. At the last stage, the mixture was transferred to an autoclave which was the put into an oil pan and continuously stirred at a temperature of  $90^\circ\text{C}$  for 5 hours. The products in a form of a solid was filtered using vacuum filter and then washed with water three times and with ethanol once. The clean product was dried at  $80^\circ\text{C}$  overnight.

Repeat above experiment at different temperature of  $60^\circ\text{C}$ ,  $120^\circ\text{C}$ .

## 2.3. Characterization

The powder X-ray diffraction (XRD) patterns of Fe-BTC/GO composites were recorded on a Shimadzu XRD-6100 analyzer with Cu  $\text{K}\alpha$  radiation ( $1.5417\text{\AA}$ ). Transmission electron microscopy (TEM) was conducted using HITACHI- H-7500. Surface area of samples were determined on Quantachrome Instruments version 3.0 at 77 K and using  $\text{N}_2$  adsorbate. The functional groups of the samples were investigated with Fourier transform infrared spectroscopy (FTIR), (FT-IR 6700-Thermo Nicolet-ThermoElectro). Energy-dispersive X-ray spectroscopy (EDX) using JEOL JSM 6500F. Concentrations of RR195 in the solutions were determined using a UV-vis spectrophotometer (LAMBDA 35 UV/Vis).

## 2.4. Photo-Fenton reaction

Pyrex glass bottles of 50 ml solution containing RR195 (conc. of 100 mg/l), Fe-BTC/GO composite (conc. of 300 mg/l), and  $\text{H}_2\text{O}_2$  (conc. of 136 mg/l) were used as batch reactors. Simulated sunlight irradiation used UV-A range lamps (4 lamps, power of 15 W for each lamp). The emission spectrum between 400 nm and 800 nm followed the solar spectrum. Photo-Fenton reaction of RR195 was carried out under a stirring condition, at room temperature ( $25^\circ\text{C}$ ) and a pH of 3. Samples were collected at different reaction times (min). Concentrations of RR195 were determined using a Lambda 35 UV-vis spectrophotometer and calibration was based on band intensities at 542 nm.

## 3. RESULTS AND DISCUSSION

### 3.1. Material characteristics

#### 3.1.1. XRD analysis

XRD patterns of GO and Fe-BTC/GO composites are presented in figure 1. In the XRD pattern of the GO sample, the sharp and intense peak at  $2\theta$  of 12 assigned to the plane of [0 0 1] belonging to GO sheets [11]. In the XRD pattern of Fe-BTC, the main diffraction peaks appear at  $2\theta$  of 24; 33.1; 35 which are identical to those reported for the Fe-BTC phase [21]. In the XRD pattern of Fe-BTC/GO, typical peaks belonging to Fe-BTC appear but the peak of  $2\theta$  of 12, represent for the GO still configuration structure but the peak is shrunk with GO materials. This can be explained that Fe-BTC crystals may be well dispersed within the inter layers of GO sheets. Two samples of Fe-BTC/GO which were synthesized at  $60^\circ\text{C}$  and  $90^\circ\text{C}$  showed sharp peaks. The peak intensity of the Fe-BTC/GO sample received at  $90^\circ\text{C}$  was higher than the Fe-BTC/GO sample at  $60^\circ\text{C}$  and  $120^\circ\text{C}$ . Fe-BTC/GO at  $120^\circ\text{C}$  still exhibits characteristic peaks of Fe-BTC but the peaks are jammed, unbalanced due to unstable structure. The X-ray diffraction spectra showed high purity Fe-BTC/GO at  $90^\circ$ .

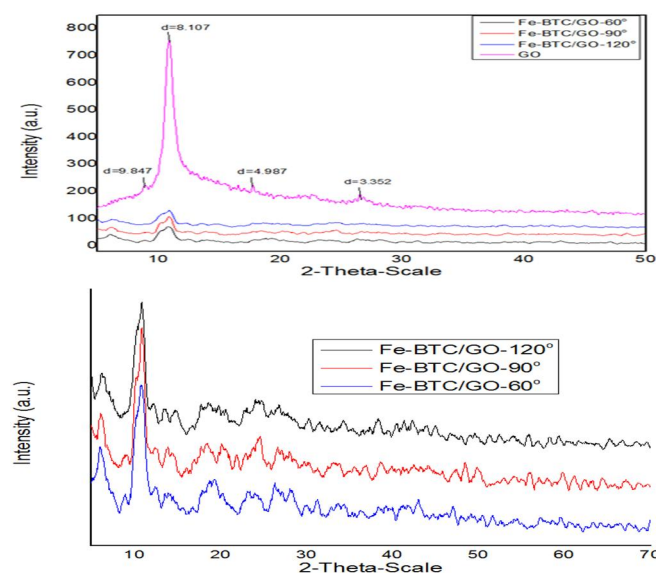


Figure 1. XRD patterns of GO and Fe-BTC/GO composites

#### 3.1.2. EDX analysis

Table 1. Elements of elements in Fe-BTC/GO composites

Element	Fe-BTC/GO (at $60^\circ\text{C}$ )		Fe-BTC/GO (at $90^\circ\text{C}$ )		Fe-BTC/GO (at $120^\circ\text{C}$ )	
	%Mass	%Atom	%Mass	%Atom	%Atom	%Mass
C	64.69	72.23	62.48	71.94	67.11	74.74
O	29.94	25.44	30.41	26.29	29.11	24.34
Fe	5.24	1.28	7.02	1.74	3.67	0.88
Cl	0.14	0.05	0.08	0.03	0.11	0.04
Total	100	100	100	100	100	100

To investigate the chemical composition of Fe-BTC/GO, EDX analysis was performed. The EDX result (Table 1) of Fe-BTC/GO shows the presence of iron. The iron content (Fe) in the Fe-BTC composite (3.67-7.02% mass) was quite close to the initial calculation of 9% Fe applied to the material, where Fe-BTC/GO 90°C contained the largest Fe content (7.02%).

3.1.3. TEM analysis

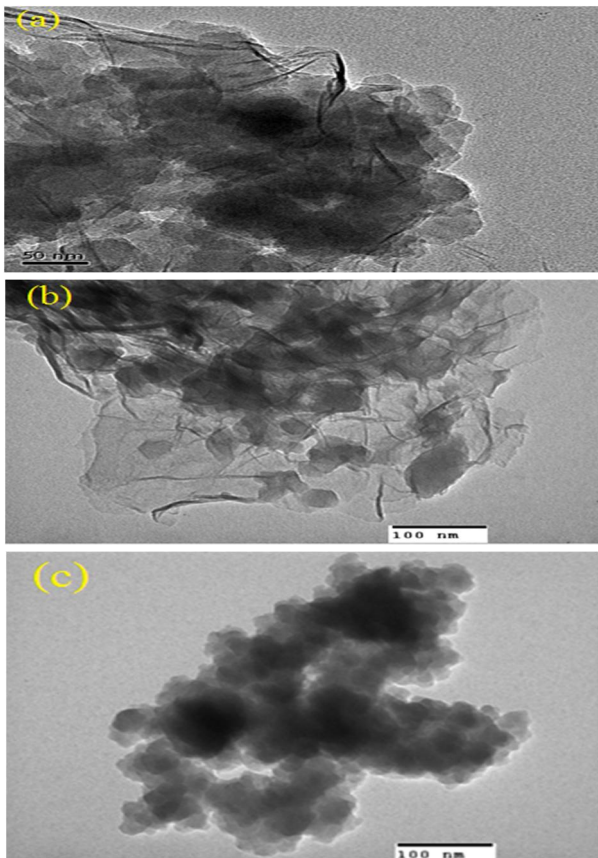


Figure 2. TEM images of Fe-BTC/GO composites 60° (a), 90° (b), 120° (c)

The TEM image of Fe-BTC/GO 60°C composite is illustrated in figure 2(a). As observed in figure 2(a), nano Fe-BTC particles were dispersed evenly on the GO layer grade and the size of the nano particle was 20-50 nm. Figure 2(b) is the TEM image of Fe-BTC/GO synthesized at 90°C. The image shows that the Fe-BTC nano particles were dispersed evenly on the GO surface layers, the size of the particles ranging from 10 to 20 nm. However, there were still small amount of Fe-BTC clusters in range of 40 to 60 nm. In fig. 2(c), the TEM image of Fe-BTC/GO synthesized at 120°C shows that the Fe-BTC nanoparticles were clumped and dispersed unevenly on GO's surface layers, the Fe-BTC nanoparticle size was in the range of 40-70 nm.

3.1.4. N<sub>2</sub> adsorption - desorption isotherm analysis (BET)

N<sub>2</sub> adsorption-desorption isotherm (BET) of Fe-BTC/GO composite is shown in figure 3, the N<sub>2</sub> adsorption-desorption curve of Fe-BTC/GO displayed the type IV isotherms with hysteresis corresponding to the capillary condensation, which is typical for mesoporous material [17].

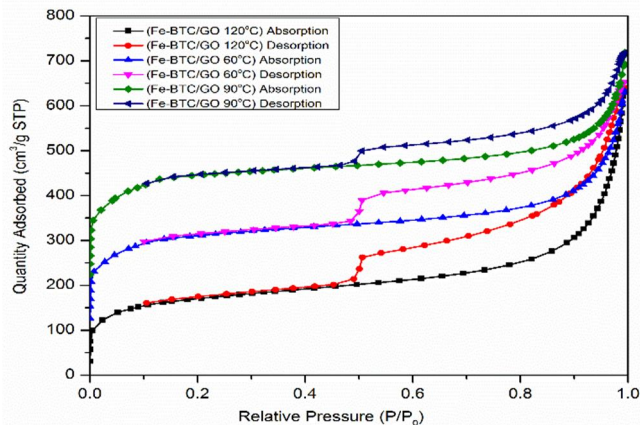


Figure 3. BET of Fe-BTC/GO composite

Table 2. Characteristics BET analysis of Fe-BTC/GO materials

Materials	S <sub>BET</sub> (m <sup>2</sup> /g)	V <sub>po</sub> (cm <sup>3</sup> /g)	D <sub>BH</sub> (nm)
Fe-BTC/GO (at 60°C)	683.15	0.712	7.56
Fe-BTC/GO (at 90°C)	786.13	0.626	5.92
Fe-BTC/GO (at 120°C)	566.07	0.887	11.31

It can be seen on the table 2 that the Fe-BTC/GO 90°C had the largest surface area (786.13 m<sup>2</sup>/g)

3.1.5. FTIR analysis

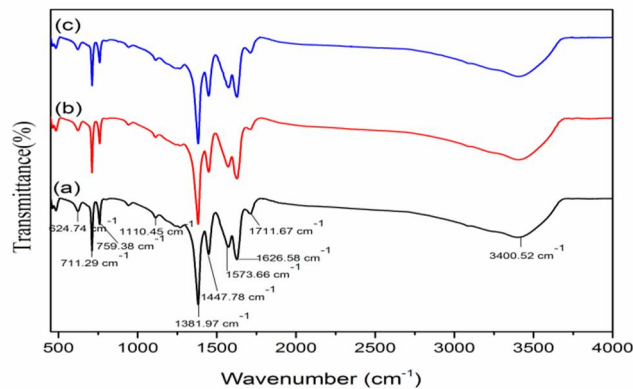


Figure 4. FTIR spectra of Fe-BTC/GO synthesized at (a) 60°C, (b) 90°C, and (c) 120°C

To identify the functional groups of the Fe-BTC/GO sample, FTIR spectra of Fe-BTC/GO synthesized at different temperature are shown in figure 4. The characteristic absorption bands of the Fe-BTC/GO sample presented at 1626, 15733, 1447, 1382, 1110, and 759 cm<sup>-1</sup>, which are assigned to carboxylate group vibrations [18, 19]. The broad bands centered at 3440 cm<sup>-1</sup> are associated with the stretching vibrations of O-H from the water adsorbed on the surface. The two sharp bands at 1250 and 1200 cm<sup>-1</sup> are attributed to asymmetric (vas (C-O)) and symmetric (vs (C-O)) vibrations of carboxyl groups, respectively. This result confirms the presence of the tricarboxylate ligands within the Fe-BTC/GO material. The bands at 759 cm<sup>-1</sup> correspond to C-H bending vibrations of benzene. The intense bands at 624 cm<sup>-1</sup> are assigned to Fe-O vibrations [18, 20], indicating the interaction between Fe-BTC and GO.

### 3.2. Photo-Fenton-like process in RR195 degradation

#### 3.2.1. Investigation of the degradation of the RR195 on samples

To investigate the photocatalytic activity of Fe-BTC/GO for degradation in aqueous solution, the RR195 was chosen model molecule. This is a commercial product often used in textile dyeing. It is well known that this reactive dye is relatively stable and hard to be degraded.

Evaluation of the rate of reactive dyestuffs was conducted under the following conditions: RR195 concentration of 100 mg/L; catalytic concentration of 0.3 g/L; H<sub>2</sub>O<sub>2</sub> concentration of 0.4 mL/100 mL; pH of 5.5; reaction temperature at 25°C and lighting. Performed with three modified catalysts at temperatures of 60°C, 90°C, 120°C.

Figure 5 shows that after 120 minutes, the RR195 concentration was 91% and 92% which were lower than the original concentration when using Fe-BTC/GO 60°C and Fe-BTC/GO 90°C composites, respectively. At the same time, dye decomposition time of Fe-BTC/GO-120°C was longer than that of other materials, even up to 150 minutes.

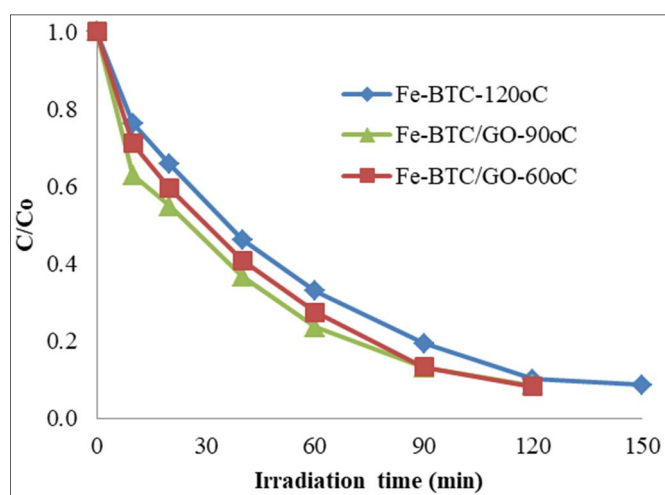


Figure 5. RR195 dye decomposition rate of Fe-BTC/GO denatured at 60°C, 90°C, 120°C

#### 3.2.2. Catalyst Activity

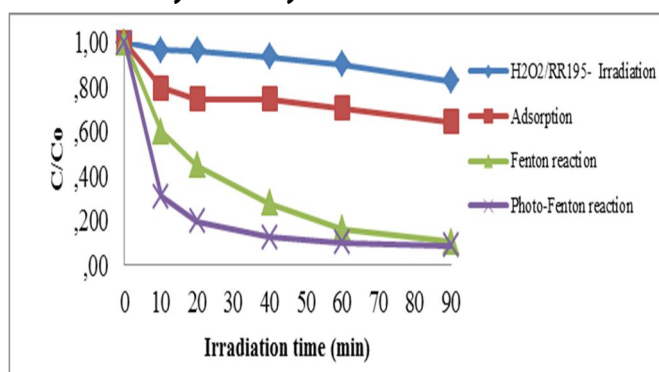


Figure 6. Plot of RR195 conversions as a function of irradiation time over the Fe-BTC/GO (at 90°C) composite at different conditions: blank, adsorption, Fenton process, photo-Fenton process

From the experimental studies of conditions influencing the reaction yield, we choose the optimum conditions as follows: RR195 initial concentration 100ppm (100mg/L), H<sub>2</sub>O<sub>2</sub> concentration 0.05 mL/100 mL; Catalytic concentration Fe-BTC/GO (at 90°C) 0.3 g/L; pH 3; temperature 25°C.

It is well known that to evaluate photo catalytic activity the contribution of adsorption capacity should be considered. As observed in figure 6, after 90 min, RR195 adsorption in the dark reached the C/Co equilibrium and then decreased to 35.67%. At the blank conditions, consisting of reactant, oxidant, and simulated sunlight and in the absence of catalyst, RR195 conversion was negligible.

In the Fenton process (in the presence of catalyst, H<sub>2</sub>O<sub>2</sub>) after 90 min of reaction, C/Co decreased to the value of 89% but in the photo-Fenton process (in the presence of catalyst, H<sub>2</sub>O<sub>2</sub>, simulated sunlight irradiation) C/Co decreased to 92%. From these results, it is clear that the novel Fe-BTC/GO composite can be used as a highly efficient photocatalyst.

### 4. CONCLUSIONS

The Fe-BTC/GO composite was successfully prepared by hydrothermal method without using organic solvent. The Fe-BTC/GO composite synthesized is novel.

The optimize temperature of the synthesis process was estimated to be 90°C. The results of the XRD and FT-IR spectrum analyzes, suggesting the Fe-BTC crystals can be dispersed and included in the links of the GO classes. From N<sub>2</sub> adsorption result, it reveals the mesoporous structure of the Fe-BTC/GO composite with mesopore volume (0.626 cm<sup>3</sup>.g<sup>-1</sup>). From TEM images, the Fe (III) oxo clusters in the Fe-BTC/GO composite have a small size of 10-20 nm.

In the photocatalytic degradation of RR195 from aqueous solution, the novel Fe-BTC/GO composite exhibited highly efficient photocatalytic activity. This result opens high application potential of a new group of photocatalysts in the degradation of organic compounds from aqueous solutions.

**Acknowledgements:** This work was financial supported by the VAST (code: VAST.07.01/18-19)

### REFERENCES

- [1]. Cook T R, Zheng Y R and Stang P J. Metal-organic frameworks and self-assembled supramolecular coordination complexes: comparing and contrasting the design, synthesis, and functionality of metal-organic materials, *Chem. Rev.* **2013**, *113* 734–77.
- [2]. Tuan A et al. Arsenic removal from aqueous solutions by adsorption using novel MIL-53(Fe) as a highly efficient adsorbent, *RSC Adv.* **2015**, *5* 5261–8.
- [3]. Wu H, Gong Q, Olson D H and Li J. Commensurate adsorption of hydrocarbons and alcohols in microporous metal organic frameworks, *Chem. Rev.* **2012**, *112* 836–68.

[4]. Liu K, Gao Y, Liu J, Wen Y, Zhao Y, Zhang K and Yu G. Photoreactivity of metal-organic frameworks in aqueous solutions: metal dependence of reactive oxygen species production *Environ. Sci. Technol.*, **2016**, *50* 3634–40.

[5]. Horcajada P, Gref R, Baati T, Allan P K, Maurin G, Couvreur P, Férey G, Morris R E and Serre C. Metal-organic frameworks in biomedicine, *Chem. Rev.*, **2012**, *112* 1232–68.

[6]. Xamena F, Corma A and Garcia H. Applications for metal-organic frameworks (MOFs) as quantum dot semiconductors *J. Phys. Chem. Rev.*, **2007**, *111* 80–5.

[7]. Alvaro M, Carbonell E, Ferrer B, Xamena F and Garcia H. Semiconductor behavior of a metal-organic framework (MOF), *Chem. Eur. J.*, **2007**, *13* 5106.

[8]. Jahan M, Bao Q, Yang J-X and Loh K P. Structure-directing role of graphene in the synthesis of metal-organic framework nanowire, *J. Am. Chem. Soc.*, **2010**, *132* 14487–95.

[9]. Shekka O, Roques N, Mugnaini V, Munuera C, Ocal C, Veciana J and Woll C. Grafting of monocarboxylic substituted polychlorotriphenylmethyl radicals onto a COOH-functionalized self-assembled monolayer through copper (II) metal ions, *Langmuir*, **2008**, *24* 6640–8.

[10]. Hermes S, Zacher D, Baunemann A, Woll C and Fischer R A. Selective growth and MOCVD loading of small single crystals of MOF-5 at alumina and silica surfaces modified with organic self-assembled monolayers, *Chem. Mater.*, **2007**, *19* 2168–73.

[11]. Bandosz T J and Petit C. MOF/graphite oxide hybrid materials: exploring the new concept of adsorbents and catalysts, *Adsorption*, **2011**, *17* 5–16.

[12]. Petit C and Bandosz T J. Exploring the coordination chemistry of MOF-graphite oxide composites and their applications as adsorbents, *Dalton Trans.*, **2012**, *41* 4027–35.

[13]. Park S et al. Aqueous suspension and characterization of chemically modified graphene sheets, *Chem. Mater.*, **2008**, *20* 6592–4.

[14]. Zhu Y, Murali S, Stoller M D, Velamakanni A, Piner R D and Ruoff R S. Microwave assisted exfoliation and reduction of graphite oxide for ultracapacitors *Carbon*, *Chem. Eur.*, **2010**, *48* 2118–22.

[15]. Wang H, Yuan X, Wu Y, Zeng G, Chen X, Leng L and Li H. Synthesis and applications of novel graphitic carbon nitride/ metal-organic frameworks mesoporous photocatalyst for dyes removal original, *Appl. Catal. B.*, **2015**, *174* 445–54.

[16]. Jia Jia, Fujian Xu, Zhou Long, Xiandeng Hou and Michael J. Sepaniak. Metal-organic framework MIL-53(Fe) for highly selective and ultrasensitive direct sensing of MeHg<sup>+</sup>, *Chem. Commun.*, **2013**, *49*, pp. 4670–4672.

[17]. Peng L, Zhang J, Li J, Han B, Xue Z and Yang G *Chem. Commun.*, **2012**, *48* 8688.

[18]. Vuong G-T, Pham M-H and Do T-O. Direct synthesis and mechanism of the formation of mixed metal Fe<sub>2</sub>Ni-MIL-88B, *CrystEngComm*, **2013**, *15* 9694–703.

[19]. Ai L, Zhang C, Li L and Jiang J. Iron terephthalate metal-organic framework: Revealing the effective activation of hydrogen peroxide for the degradation of organic dye under visible light irradiation, *Appl. Catal. B.*, **2014**, *148–9* 191–200.

[20]. Gardella J A, Ferguson S A and Chin R L. The shakeup satellites for the  $\pi^*-\pi$  analysis of structure and bonding in aromatic polymers by x-ray photoelectron spectroscopy, *Appl. Spectrosc.*, **1986**, *40* 224–32.

[21]. Chulwoo Park, Jinhwan Jung, Chul Wee Lee, Joungmo Cho. Synthesis of Mesoporous  $\alpha$ -Fe<sub>2</sub>O<sub>3</sub> Nanoparticles by Non-ionic Soft Template and Their Applications to Heavy Oil Upgrading, *Catalysis Today*, **2015**, *271*, 98–110.